

A Nonlinear Model-Based Wind Velocity Observer for Unmanned Aerial Vehicles

Kasper T. Borup Thor I. Fossen Tor A. Johansen

*Department of Engineering Cybernetics
Norwegian University of Science and Technology
7491 Trondheim, Norway
E-mail: kasper.borup@ntnu.no / thor.fossen@ntnu.no /
tor.arne.johansen@itk.ntnu.no*

Abstract: This paper presents an exponentially stable nonlinear wind velocity observer for fixed-wing unmanned aerial vehicles (UAVs). The observer uses a model of the aircraft combined with a GNSS-aided inertial navigation system (INS). The INS uses an attitude observer together with a pitot static probe measuring dynamic pressure in the longitudinal direction as well as the airspeed. The observer is able to estimate the wind velocity and from this compute the relative velocity, which directly contains information about the angle of attack (AOA) and sideslip angle (SSA). The nonlinear observer is also able to estimate the scaling factor of the pitot static probe measurement and there are no requirements on persistence of excitation (PE) of the UAV maneuvers. The computational footprint is smaller than the conventional Kalman filter, which makes the algorithm well suited for embedded systems. The designed observer is proven exponentially stable under stable flight and through simulations it is verified that the estimates converge to the true values of a realistic wind velocity when there are no model errors.

Keywords: Nonlinear Observers, Wind Velocity, Unmanned Aerial Vehicles, Inertial Navigation Systems

1. INTRODUCTION

The ability to correctly estimate the wind and relative velocity for a fixed-wing UAV is very important. Knowledge of the wind velocity can be exploited in the control system where the wind can be treated as a disturbance and from the relative velocity both the AOA and SSA are directly computable. The AOA and SSA contain useful information related to the performance and safety of the aircraft, e.g. the value of the AOA is directly related to whether the wing is under stall conditions which leads to turbulent air flow and a considerable drop in the wing-produced lift force (Beard and McLain [2012]). Autonomous landing operations also require information about the wind. Larger fixed-wing aircraft are often equipped with sensors, such as vanes and multi-hole pitot probes, that provide measurements of the wind velocity along with the AOA and SSA. For a small UAV, this solution is expensive and impractical due to space limitations, weight constraints and increased power consumption. Yet having the information about the wind would be useful for the relatively inexpensive aircraft to perform autonomous missions such as a payload deployment or pickup, or a precise landing in a small net aboard a ship. It is therefore highly desirable to have a wind and relative velocity observer only utilizing measurements obtained by the standard sensor suite equipped on a UAV, an inertial measurement unit (IMU), a Global Navigation Satellite System (GNSS) receiver (Beard and McLain [2012], Farrell [2008]), and a pitot static probe in conjunction with a differential pressure sensor supplying an air speed measurement (Beard and McLain

[2012]).

When designing an observer for a nonlinear system a common approach is to use the Extended Kalman Filter (EKF) (Brown [1972]). This approach has been used for developing wind velocity observers based on the kinematic equations in combination with an aerodynamic model of the aircraft, e.g. Kumon et al. [2005], Long and Song [2009], Langelaa et al. [2011], Ramprasadh and Arya [2012], and Cho et al. [2013]. Rodriguez et al. [2007] present a method for estimating wind velocity for a miniature aerial vehicle (MAV) by using optical flow. Paces et al. [2010] proposes a twin differential sensor setup for estimating the AOA and SSA. An EKF structure with a pitot static probe is also used by Hansen and Blanke [2014] for detecting sensor failure and Lie and Gebre-Egziabher [2013] propose an EKF for estimating the wind velocity without the pitot static probe air speed measurement. A model-free wind velocity observer has been proposed by Cho et al. [2011] and Rhudy et al. [2013] avoiding the aircraft model. Johansen et al. [2015] have also developed a model-free observer, which is able to estimate the pitot static probe correction factor and thus provide online calibration and fault detection of the airspeed sensor. The model-free observer requires that the yaw and pitch motions are persistently excited (PE) in order to ensure convergent estimates. An extension that also uses IMU measurements and lift coefficient estimation is given in Wenz et al. [2016]. The observer in this paper removes the PE condition for the price of using a relatively simple aircraft model to obtain convergent estimates.

1.1 Contributions of this paper

The main contribution of the paper is a nonlinear observer that provides exponential stability and convergent estimates of wind velocity from which estimates of AOA and SSA can be derived. The observer utilizes a standard UAV sensor suite combined with a relatively simple aerodynamic model of the aircraft, which is updated using propeller revolutions and pitot static probe measurements. An advantage of the observer is that no maneuvers or requirements for PE are needed. A potential disadvantage is that model errors may give errors in the estimates. Another contribution of the paper is the compact representation of the small aircraft model of Beard and McLain [2012] using the matrix-vector representation of Fossen [2011]. For the proof, the aerodynamic forces were divided into a stabilizing linear term and a vector of the remaining nonlinear aerodynamic forces with physical properties such as energy dissipation, which can be exploited when constructing the Lyapunov function for observer error dynamics. Finally, the nonlinear observer is validated through simulation using a small fixed-wing UAV exposed to wind.

1.2 Notation and preliminaries

For a vector or matrix \mathbf{X} , \mathbf{X}^\top denotes its transpose. The operator $\|\cdot\|$ denotes the Euclidean norm for vectors and the Frobenius norm for matrices. For a vector $\mathbf{x} \in \mathbb{R}^3$, $\mathbf{S}(\mathbf{x})$ denotes the skew-symmetric matrix:

$$\mathbf{S}(\mathbf{x}) = \begin{bmatrix} 0 & -x_3 & x_2 \\ x_3 & 0 & -x_1 \\ -x_2 & x_1 & 0 \end{bmatrix}$$

The $n \times n$ identity matrix is denoted by $\mathbf{I}_{n \times n}$ and the $m \times n$ zero element matrix by $\mathbf{0}_{m \times n}$. Vectors in the body-fixed (BODY) and North-East-Down (NED) coordinate frames are denoted by the superscripts b and n , respectively. Consequently, the linear velocity vector satisfies $\mathbf{v}^n = \mathbf{R}\mathbf{v}^b$ where $\mathbf{R} \in \text{SO}(3)$ is the rotation matrix from BODY to NED.

1.3 Problem formulation

The UAV's velocity over ground can be expressed as the sum of the relative velocity and the wind velocity according to:

$$\mathbf{v}^b = \mathbf{v}_r^b + \mathbf{v}_w^b \quad (1)$$

where $\mathbf{v}^b = [u, v, w]^\top$ is the UAV's linear velocity vector, $\mathbf{v}_r^b = [u_r, v_r, w_r]^\top$ is the relative velocity vector and $\mathbf{v}_w^b = [u_w, v_w, w_w]^\top$ is the wind velocity vector. The goal is to estimate \mathbf{v}_w^b and \mathbf{v}_r^b , since the airspeed V_a , AOA and SSA are recognized as:

$$V_a = \sqrt{u_r^2 + v_r^2 + w_r^2} > 0 \quad (2)$$

$$\alpha = \tan^{-1} \left(\frac{w_r}{u_r} \right) \quad (3)$$

$$\beta = \sin^{-1} \left(\frac{v_r}{V_a} \right) \quad (4)$$

2. UAV RIGID-BODY KINETICS

By application of *Euler's first and second axioms* the rigid-body kinetics for the translational and rotational dynamics of a rigid body is (Fossen [2011])

$$m(\dot{\mathbf{v}}^b + \mathbf{S}(\boldsymbol{\omega}^b)\mathbf{v}^b) = \mathbf{f}^b \quad (5)$$

$$\mathbf{J}\dot{\boldsymbol{\omega}}^b - \mathbf{S}(\mathbf{J}\boldsymbol{\omega}^b)\boldsymbol{\omega}^b = \mathbf{m}^b \quad (6)$$

where m is the mass of the vehicle, $\boldsymbol{\omega}^b = [p, q, r]^\top$ is the body-fixed angular velocities, $\mathbf{J} \in \mathbb{R}^{3 \times 3}$ is the symmetric inertia tensor and \mathbf{f}^b and \mathbf{m}^b are the forces and moments on the vehicle. In Beard and McLain [2012] it is shown that a small aircraft can be modeled by (5) and (6) where

$$\mathbf{J} = \begin{bmatrix} J_x & 0 & -J_{xz} \\ 0 & J_y & 0 \\ -J_{xz} & 0 & J_z \end{bmatrix} \quad (7)$$

is a matrix of products and moments of inertia. The aircraft forces and moments can be approximated by the following formula (Beard and McLain [2012]):

$$\begin{bmatrix} \mathbf{f}^b \\ \mathbf{m}^b \end{bmatrix} = \frac{1}{2}\rho V_a^2 S \begin{bmatrix} -C_D(\alpha) \cos(\alpha) + C_L(\alpha) \sin(\alpha) \\ C_{Y_0} + C_{Y_\beta} \beta \\ -C_D(\alpha) \sin(\alpha) - C_L(\alpha) \cos(\alpha) \\ b(C_{l_0} + C_{l_\beta} \beta + C_{l_{\delta_a}} \delta_a + C_{l_{\delta_r}} \delta_r) \\ c(C_{m_0} + C_{m_\alpha} \alpha + C_{m_{\delta_e}} \delta_e) \\ b(C_{n_0} + C_{n_\beta} \beta + C_{n_{\delta_a}} \delta_a + C_{n_{\delta_r}} \delta_r) \end{bmatrix} + \frac{1}{2}\rho V_a^2 S \begin{bmatrix} C_{X_q}(\alpha) \frac{c}{2V_a} q + C_{X_{\delta_e}}(\alpha) \delta_e \\ C_{Y_p} \frac{b}{2V_a} p + C_{Y_r} \frac{b}{2V_a} r + C_{Y_{\delta_a}} \delta_a + C_{Y_{\delta_r}} \delta_r \\ C_{Z_q}(\alpha) \frac{c}{2V_a} q + C_{Z_{\delta_e}}(\alpha) \delta_e \\ b(C_{l_p} p + C_{l_r} r) \frac{b}{2V_a} \\ c(C_{m_q} q) \frac{b}{2V_a} \\ b(C_{n_p} p + C_{n_r} r) \frac{b}{2V_a} \end{bmatrix} + \begin{bmatrix} -mg \sin \theta \\ mg \cos \theta \sin \phi \\ mg \cos \theta \cos \phi \\ 0 \\ 0 \\ 0 \end{bmatrix} + \begin{bmatrix} \frac{1}{2}\rho S_{\text{prop}} C_{\text{prop}} \left((k_{\text{motor}} \delta_t)^2 - V_a^2 \right) \\ 0 \\ 0 \\ -k_{T_p} (k_\Omega \delta_t)^2 \\ 0 \\ 0 \end{bmatrix} \quad (8)$$

where ρ is the density of air, and θ and ϕ are pitch and roll angles. The aerodynamic lift and drag coefficients, $C_L(\alpha)$ and $C_D(\alpha)$, and the aerodynamic force coefficients are nonlinear functions of AOA:

$$C_{X_q}(\alpha) \triangleq -C_{D_q} \cos(\alpha) + C_{L_q} \sin(\alpha)$$

$$C_{X_{\delta_e}}(\alpha) \triangleq -C_{D_{\delta_e}} \cos(\alpha) + C_{L_{\delta_e}} \sin(\alpha)$$

$$C_{Z_q}(\alpha) \triangleq -C_{D_q} \sin(\alpha) - C_{L_q} \cos(\alpha)$$

$$C_{Z_{\delta_e}}(\alpha) \triangleq -C_{D_{\delta_e}} \sin(\alpha) - C_{L_{\delta_e}} \cos(\alpha)$$

while C_{Y_0} , C_{Y_β} , C_{l_0} , C_{l_β} , $C_{l_{\delta_a}}$, C_{n_0} , C_{n_β} , $C_{n_{\delta_a}}$, $C_{n_{\delta_r}}$, C_{Y_p} , C_{Y_r} , $C_{Y_{\delta_a}}$, C_{l_p} , C_{l_r} , C_{m_q} , C_{n_p} , C_{n_r} , and C_{prop} are constant aerodynamic coefficients. $\boldsymbol{\delta} = [\delta_a, \delta_e, \delta_r, \delta_t]$ are the control signals of the aileron deflection, elevator deflection, rudder deflection and throttle deflection. The area of the wing is given by S , the propeller area is S_{prop} , b is the wing span, and c is the mean aerodynamic chord of the wing. k_{motor} is the efficiency of the motor and k_{T_p} and k_Ω are constants that relate the throttle deflection δ_t to the moment opposite the propeller rotation.

3. MATRIX-VECTOR FORM AIRCRAFT MODEL

The aircraft model of Beard and McLain [2012] can be expressed in matrix-vector form according to (Fossen [2011])

$$\mathbf{M}_{RB} \dot{\boldsymbol{\nu}} + \mathbf{C}_{RB}(\boldsymbol{\nu}) \boldsymbol{\nu} = \boldsymbol{\tau}_{RB} \quad (9)$$

where $\boldsymbol{\nu} = [\boldsymbol{v}^b; \boldsymbol{\omega}^b]$ is the 6-DOF generalized velocity vector. The rigid-body mass matrix \boldsymbol{M}_{RB} and rigid-body Coriolis and centripetal matrix $\boldsymbol{C}_{RB}(\boldsymbol{\nu})$ are given by

$$\boldsymbol{M}_{RB} = \begin{bmatrix} m\boldsymbol{I}_{3\times 3} & \mathbf{0}_{3\times 3} \\ \mathbf{0}_{3\times 3} & \boldsymbol{J} \end{bmatrix} \quad (10)$$

$$\boldsymbol{C}_{RB}(\boldsymbol{\nu}) = \begin{bmatrix} m\boldsymbol{S}(\boldsymbol{\omega}^b) & \mathbf{0}_{3\times 3} \\ \mathbf{0}_{3\times 3} & -\boldsymbol{S}(\boldsymbol{J}\boldsymbol{\omega}^b) \end{bmatrix} \quad (11)$$

The generalized vector of external forces and moments is $\boldsymbol{\tau}_{RB} = [\boldsymbol{f}^b; \boldsymbol{m}^b]$. The wind velocity is assumed irrotational and steady relative to the Earth. The generalized wind velocity of an irrotational fluid is

$$\boldsymbol{\nu}_w = \underbrace{[u_w, v_w, w_w, 0, 0, 0]^\top}_{\boldsymbol{v}_w^b} \quad (12)$$

and the generalized relative velocity vector $\boldsymbol{\nu}_r = \boldsymbol{\nu} - \boldsymbol{\nu}_w$. Since $\boldsymbol{v}_w^n = \boldsymbol{R}\boldsymbol{v}_w^b$, then under assumption of steady wind ($\dot{\boldsymbol{v}}_w^n = \mathbf{0}$), we get

$$\dot{\boldsymbol{v}}_w^n = \dot{\boldsymbol{R}}\boldsymbol{v}_w^b + \boldsymbol{R}\dot{\boldsymbol{v}}_w^b = \mathbf{0} \quad (13)$$

where $\dot{\boldsymbol{R}} = \boldsymbol{R}\boldsymbol{S}(\boldsymbol{\omega}^b)$. Consequently,

$$\dot{\boldsymbol{v}}_w^b = \boldsymbol{S}(\boldsymbol{\omega}^b)\boldsymbol{v}_w^b \quad (14)$$

This leads to the property

$$\boldsymbol{M}_{RB}\dot{\boldsymbol{\nu}}_w + \boldsymbol{C}_{RB}(\boldsymbol{\nu}_r)\boldsymbol{\nu}_w = \mathbf{0} \quad (15)$$

which is easily verified by expanding the matrices \boldsymbol{M}_{RB} and \boldsymbol{C}_{RB} . Hence,

$\boldsymbol{M}_{RB}\dot{\boldsymbol{\nu}} + \boldsymbol{C}_{RB}(\boldsymbol{\nu})\boldsymbol{\nu} = \boldsymbol{M}_{RB}[\dot{\boldsymbol{\nu}}_r + \dot{\boldsymbol{\nu}}_w] + \boldsymbol{C}_{RB}(\boldsymbol{\nu}_r)[\boldsymbol{\nu}_r + \boldsymbol{\nu}_w]$ and finally, by inserting (15) we get

$$\boldsymbol{M}_{RB}\dot{\boldsymbol{\nu}} + \boldsymbol{C}_{RB}(\boldsymbol{\nu})\boldsymbol{\nu} = \boldsymbol{M}_{RB}\dot{\boldsymbol{\nu}}_r + \boldsymbol{C}_{RB}(\boldsymbol{\nu}_r)\boldsymbol{\nu}_r \quad (16)$$

Notice that (16) is the equivalent to Property 8.1 in Fossen [2011]. The dynamics of the relative velocity $\boldsymbol{\nu}_r$ can finally be expressed as:

$$\boldsymbol{M}_{RB}\dot{\boldsymbol{\nu}}_r + \boldsymbol{C}_{RB}(\boldsymbol{\nu}_r)\boldsymbol{\nu}_r = \boldsymbol{\tau}_{RB} \quad (17)$$

4. NONLINEAR WIND VELOCITY OBSERVER

The following section presents the wind velocity observer.

4.1 Measurements

The proposed wind observer and the GNSS-aided inertial navigation system (INS), which consists of an IMU and an attitude observer, forms a cascade as shown in Figure 1. The following measurements are needed to implement the observer:

- An attitude measurement, typically represented as Euler angles or unit quaternions used to compute the rotation matrix \boldsymbol{R} .
- Measurement of the airspeed V_a
- Airspeed sensor measuring the relative longitudinal velocity $u_r^m > 0$, which relates to the relative longitudinal velocity $u_r = \gamma u_r^m$ by an unknown positive scaling factor γ .
- An angular velocity (rate gyro) measurement $\boldsymbol{\omega}^b$ which has been compensated for gyro drift and bias.
- The control surface deflections $\delta_t, \delta_a, \delta_e$ and δ_r .
- The UAV velocity \boldsymbol{v}^n in NED measured by the GNSS.

A block diagram of the observer is shown in Figure 1.

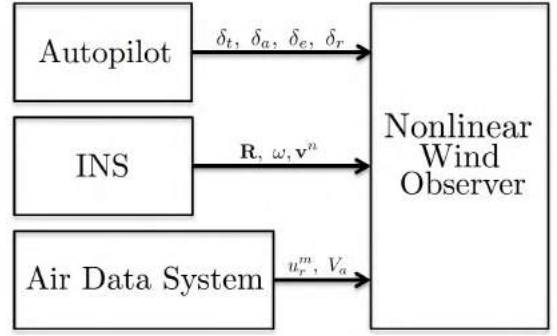


Fig. 1. Block diagram showing the cascaded structure of the observer including the signals used in the wind velocity observer.

4.2 Assumptions

The key assumptions needed to prove exponential stability are:

- The INS GNSS measurements \boldsymbol{R} , $\boldsymbol{\omega}^b$ and \boldsymbol{v}^n are smooth bounded signals. Hence, these signals will be treated as time-varying known signals and not states in the observer. This implies that the observer error dynamics become nonautonomous.
- The wind velocity vector is constant (or at least slowly varying) such that $\dot{\boldsymbol{v}}_w^n = \mathbf{0}$.
- The sensor scaling factor γ is positive and constant (or at least slowly varying) such that $\dot{\gamma} = 0$, and the relative longitudinal velocity u_r is positive.
- The relative velocity in the lateral direction v_r is small compared to the airspeed V_a and consequently the SSA, that is β , is small.
- The lift and drag coefficient, $C_L(\alpha)$ and $C_D(\alpha)$, are linear in α , i.e. α is small.
- The aircraft and autopilot system is closed-loop stable (stable flight) and the flight envelope ensures the σ_1 , as defined in the proof in Appendix A, is positive.

4.3 Observer model

To simplify the notation, time-varying measurements will be denoted by time t when using functions, i.e.

$$\boldsymbol{R} := \boldsymbol{R}(t) \quad (18)$$

$$\boldsymbol{S}(\boldsymbol{\omega}^b) := \boldsymbol{S}(t) \quad (19)$$

Hence, the translational motion components of (17) can be written as:

$$m\dot{\boldsymbol{v}}_r^b + m\boldsymbol{S}(t)\boldsymbol{v}_r^b + m\boldsymbol{R}^\top(t)\boldsymbol{g}^n = \boldsymbol{\tau}_{\text{aero},1}(\boldsymbol{v}_r^b, t) + \boldsymbol{\tau}_{\text{aero},2}(t) \quad (20)$$

with $\boldsymbol{g}^n = [0, 0, g]^\top$. The functions below depend on the state \boldsymbol{v}_r^b and time-varying measurements represented by the argument t :

$$\begin{aligned} \boldsymbol{\tau}_{\text{aero},1}(\boldsymbol{v}_r^b, t) := & \frac{1}{2}\rho S V_a^2 \begin{bmatrix} -C_D(\alpha) \cos(\alpha) + C_L(\alpha) \sin(\alpha) \\ C_{Y_0} + C_{Y_\beta} \beta \\ -C_D(\alpha) \sin(\alpha) - C_L(\alpha) \cos(\alpha) \end{bmatrix} \\ & + \frac{1}{2}\rho S V_a^2 \begin{bmatrix} C_{X_q}(\alpha) \frac{c}{2V_a} q + C_{X_{\delta_e}}(\alpha) \delta_e - \frac{1}{S} S_{\text{prop}} C_{\text{prop}} \\ 0 \\ C_{Z_q}(\alpha) \frac{c}{2V_a} q + C_{Z_{\delta_e}}(\alpha) \delta_e \end{bmatrix} \end{aligned} \quad (21)$$

$$\boldsymbol{\tau}_{\text{aero},2}(t) := \begin{bmatrix} \frac{1}{2}\rho S_{\text{prop}} C_{\text{prop}} (k_{\text{motor}} \delta_t)^2 \\ \frac{1}{2}\rho S V_a^2 \left(C_{Y_p} \frac{b}{2V_a} p + C_{Y_r} \frac{b}{2V_a} r + C_{Y_{\delta_a}} \delta_a + C_{Y_{\delta_r}} \delta_r \right) \\ 0 \end{bmatrix} \quad (22)$$

The reason for this separation of the aerodynamic forces will become apparent in the proof.

4.4 Wind observer design

As shown in Lemma 1 in Appendix A, for small AOA and SSA the linear and nonlinear terms of $\boldsymbol{\tau}_{\text{aero},1}(\mathbf{v}_r^b, t)$ can be expressed as a sum:

$$\boldsymbol{\tau}_{\text{aero},1}(\mathbf{v}_r^b, t) := -\mathbf{D}(t)\mathbf{v}_r^b - \mathbf{d}(\mathbf{v}_r^b, t) \quad (23)$$

Hence, for a stable flight $\mathbf{D}(t) > 0$ and $\mathbf{v}_r^{b\top} \mathbf{d}(\mathbf{v}_r^b, t) \geq 0$, $\forall t \geq 0$. Furthermore, when designing the observer we assume that the nonlinear aerodynamic terms satisfy:

$$\mathbf{P} \left[\frac{\partial \mathbf{d}(\mathbf{v}_r^b, t)}{\partial \mathbf{v}_r^b} \right] + \left[\frac{\partial \mathbf{d}(\mathbf{v}_r^b, t)}{\partial \mathbf{v}_r^b} \right]^\top \mathbf{P} \geq 0, \quad \forall \mathbf{v}_r^b \in \mathbb{R}^n, t \geq 0 \quad (24)$$

where $\mathbf{P} = \mathbf{P}^\top > 0$. Then the following property (Aamo et al. [2001]) holds:

$$(\mathbf{x} - \mathbf{y})^\top \mathbf{P}(\mathbf{d}(\mathbf{x}, t) - \mathbf{d}(\mathbf{y}, t)) \geq 0, \quad \forall \mathbf{x}, \mathbf{y} \in \mathbb{R}^3, t \geq 0 \quad (25)$$

Notice that $\mathbf{d}(\mathbf{v}_r^b, t)$ depends on time-varying measurements such as gyro rates, control surfaces, airspeed etc. Consequently, Condition (24) must be satisfied for all measured signals, which are assumed to be smooth and bounded.

Proposition 1. (Nonlinear wind observer). Under the assumptions given in Section 4.2 and ineq. (24), the nonlinear observer:

$$m\dot{\hat{\mathbf{v}}}_r^b = -\mathbf{S}(t)\hat{\mathbf{v}}_r^b + \boldsymbol{\tau}_{\text{aero},1}(\hat{\mathbf{v}}_r^b, t) + \boldsymbol{\tau}_{\text{aero},2}(t) - m\mathbf{R}^\top(t)\mathbf{g}^n - K_u \mathbf{h} (\mathbf{h}^\top \hat{\mathbf{v}}_r^b - \hat{\gamma} u_r^m(t)) \quad (26)$$

$$\dot{\hat{\gamma}} = K_\gamma (\mathbf{h}^\top \hat{\mathbf{v}}_r^b - \hat{\gamma} u_r^m(t)) \quad (27)$$

$$\hat{\mathbf{v}}_w^b = \mathbf{R}^\top(t)\mathbf{v}^n - \hat{\mathbf{v}}_r^b \quad (28)$$

renders the equilibrium point $(\tilde{\mathbf{v}}_r^b, \tilde{\gamma}) = (\mathbf{0}, 0)$ globally exponentially stable (GES) if the observer gains are chosen as $K_u > 0$ and $K_\gamma = K_u u_r^m$. The vector $\mathbf{h} = [1 \ 0 \ 0]^\top$ is a selection vector, $u_r^m(t) > 0$ for all t is the pitot static probe air speed measurement in the longitudinal direction, and $\mathbf{R}(t)$, $\boldsymbol{\omega}^b(t)$ and $\mathbf{v}^n(t)$ are the INS and GNSS measurements, respectively. Notice that the airspeed measurement V_a is used in the expression for $\boldsymbol{\tau}_{\text{aero},2}(t)$ given by (22), whereas the airspeed estimate $\hat{V}_a = \|\hat{\mathbf{v}}_r^b\|$ is used in the expression for $\boldsymbol{\tau}_{\text{aero},1}(\hat{\mathbf{v}}_r^b, t)$ given by (21).

Comment on local versus global stability: The stability result is in practice local since the observer is based on the linear expressions (48)–(51) for the aerodynamic forces. The linear drag and lift coefficients $C_L(\alpha)$ and $C_D(\alpha)$ cannot describe nonlinear maneuvers such as stall, spinning etc.

Comment on the V_a measurement: Small UAVs usually measures the longitudinal airspeed u_r , but a direct measurement of V_a is usually not available. The simulations in this paper show similar results by exchanging the V_a measurement with the estimate \hat{V}_a in $\boldsymbol{\tau}_{\text{aero},2}(t)$, but no analysis has been performed to support this.

Proof: Since $\hat{\mathbf{v}}_w^b$ is algebraically related to \mathbf{v}_r^b by (28), it is only necessary to prove that the estimated states $\hat{\mathbf{v}}_r^b$ and $\hat{\gamma}$ converge to their true values. Consider the translational dynamics of the relative velocity and rewrite the correction term in terms of the error states (20) and (26) such that:

$$\begin{aligned} m\dot{\tilde{\mathbf{v}}}_r^b &= \boldsymbol{\tau}_{\text{aero},1}(\mathbf{v}_r^b, t) - \boldsymbol{\tau}_{\text{aero},1}(\hat{\mathbf{v}}_r^b, t) \\ &\quad + K_u \mathbf{h} (\mathbf{h}^\top \hat{\mathbf{v}}_r^b - \hat{\gamma} u_r^m(t)) \\ &= -(\mathbf{D}(t)\mathbf{v}_r^b - \mathbf{D}(t)\hat{\mathbf{v}}_r^b) - (\mathbf{d}(\mathbf{v}_r^b, t) - \mathbf{d}(\hat{\mathbf{v}}_r^b, t)) \\ &\quad + K_u \mathbf{h} (\mathbf{h}^\top \hat{\mathbf{v}}_r^b - u_r^m(t)\gamma + u_r^m(t)\tilde{\gamma}) \\ &= -\mathbf{D}(t)\tilde{\mathbf{v}}_r^b - (\mathbf{d}(\mathbf{v}_r^b, t) - \mathbf{d}(\hat{\mathbf{v}}_r^b, t)) \\ &\quad + K_u \mathbf{h} (u_r^m(t)\tilde{\gamma} - \mathbf{h}^\top \tilde{\mathbf{v}}_r^b) \end{aligned} \quad (29)$$

$$\dot{\tilde{\gamma}} = -K_\gamma (u_r^m(t)\tilde{\gamma} - \mathbf{h}^\top \tilde{\mathbf{v}}_r^b) \quad (30)$$

Consider the Lyapunov function candidate:

$$V = \frac{1}{2} m (\tilde{\mathbf{v}}_r^{b\top} \tilde{\mathbf{v}}_r^b + \tilde{\gamma}^2) \quad (31)$$

Hence,

$$\begin{aligned} \dot{V} &= \tilde{\mathbf{v}}_r^{b\top} (\mathbf{D}(t)^\top + \mathbf{D}(t)) \tilde{\mathbf{v}}_r^b + \tilde{\mathbf{v}}_r^{b\top} (\mathbf{d}(\mathbf{v}_r^b, t) - \mathbf{d}(\hat{\mathbf{v}}_r^b, t)) \\ &\quad + K_u (\tilde{\mathbf{v}}_r^{b\top} \mathbf{h} u_r^m(t)\tilde{\gamma} - \tilde{\mathbf{v}}_r^{b\top} \mathbf{h} \mathbf{h}^\top \tilde{\mathbf{v}}_r^b) \\ &\quad - K_\gamma (u_r^m(t)\tilde{\gamma}^2 - \tilde{\gamma} \mathbf{h}^\top \tilde{\mathbf{v}}_r^b) \\ &\leq -[\tilde{\gamma} \ \tilde{\mathbf{v}}_r^{b\top}] \mathbf{Q}(t) \begin{bmatrix} \tilde{\gamma} \\ \tilde{\mathbf{v}}_r^b \end{bmatrix} \end{aligned} \quad (32)$$

thanks to (25) and

$$\mathbf{Q}(t) := \begin{bmatrix} K_\gamma u_r^m & -K_\gamma & 0 & 0 \\ -K_u u_r^m & \rho S \sigma_1 + K_u & 0 & 0 \\ 0 & 0 & -\rho S C_{Y_\beta} & 0 \\ 0 & 0 & 0 & \rho S \sigma_1 \end{bmatrix} \quad (33)$$

where the expression for $\sigma_1 = (C_{D_0} + C_{D_{\delta_e}} \delta_e(t)) V_{a,\min} + C_{D_q} c q(t)/2$ is derived in Appendix A. To assess whether $\mathbf{Q}(t)$ is positive definite we consider the leading principal minors of the symmetric matrix $\mathbf{Q}(t) + \mathbf{Q}^\top(t)$. If the gains are chosen such that $4K_\gamma u_r^m (\rho S \sigma_1 + K_u) - (K_u u_r^m + K_\gamma)^2 > 0$ and since $\sigma_1 > 0$ and $C_{Y_\beta} < 0$ then it follows that $\dot{V} < 0$ for $\tilde{\mathbf{v}}_r^b \neq \mathbf{0}$ and $\tilde{\gamma} \neq 0$. Finally, by invoking Theorem 4.10 in Khalil [2002] the conditions for GES are easily verified. ■

Corollary 1. If the wind velocity observer (26)–(28) is in cascade with an attitude observer where the equilibrium point of the error dynamics $\hat{\mathbf{R}} = \mathbf{R} - \hat{\mathbf{R}} = \mathbf{0}$ is GES, then the nonlinear wind velocity observer (26)–(28) with \mathbf{R} exchanged with the estimate $\hat{\mathbf{R}}$ is GES.

Proof: See Appendix B. ■

5. AEROSONDE UAV STABILITY REQUIREMENTS

The stability requirements (Proposition 1) of the observer (26)–(28) can appear difficult to evaluate and a case study is therefore presented using the Aerosonde UAV (Beard and McInain [2012]). For the Aerosonde UAV the requirement $\sigma_1 > 0$ reduces to (both $C_{D_{\delta_e}}$ and C_{D_q} are zero):

$$0.03 V_{a,\min} > 0 \quad (34)$$

which clearly is satisfied. Since $C_{Y_\beta} = -0.98$ the matrix $\mathbf{D}(t) > 0$ for all $t \geq 0$. The Condition (24) can be rewritten as (see Appendix A):

$$\begin{bmatrix} \frac{\partial \mathbf{d}}{\partial \mathbf{v}_r^b} \end{bmatrix} + \begin{bmatrix} \frac{\partial \mathbf{d}}{\partial \mathbf{v}_r^b} \end{bmatrix}^\top := \rho S \begin{bmatrix} \zeta_1 & 0 & \zeta_2 \\ 0 & 0 & 0 \\ \zeta_2 & 0 & \zeta_3 \end{bmatrix} \geq 0 \quad (35)$$

where

$$\begin{aligned} \zeta_1 &= 2C_{D_\alpha} w_r + 4 \frac{1}{S} S_{\text{prop}} C_{\text{prop}} u_r + 2\eta_1 u_r / V_a \\ &\quad + 2(C_{D_0} + C_{D_{\delta_e}} \delta_e) \Delta V_a \\ \zeta_2 &= C_{D_\alpha} u_r - C_{L_\alpha} w_r + 2 \frac{1}{S} S_{\text{prop}} C_{\text{prop}} w_r \\ &\quad + (\eta_1 w_r + \eta_2 u_r) / V_a \\ \zeta_3 &= 2C_{L_\alpha} u_r + 4C_{D_\alpha} w_r + 2\eta_2 w_r / V_a \\ &\quad + 2(C_{D_0} + C_{D_{\delta_e}} \delta_e) \Delta V_a \end{aligned}$$

Hence, the inequality (24) is satisfied with $\mathbf{P} = \mathbf{I}$ for all $t \geq 0$ iff $\zeta_1 \geq 0$, $\zeta_3 \geq 0$, and $\zeta_1 \zeta_3 - \zeta_2^2 > 0$.

For $\zeta_1 > 0$:

$$0.30w_r + 0.41u_r + 0.30\Delta V_a + 0.03u_r^2/V_a - (0.28 - 0.36\delta_e(t))w_r V_a > 0 \quad (36)$$

This can be rewritten as

$$0.03u_r^2/V_a + 0.41u_r + 0.30\Delta V_a > 0.02w_r(1 - V_a) - 0.36\delta_e(t)w_r V_a \quad (37)$$

Similarly for ζ_3 we have:

$$6.90u_r + 0.06\Delta V_a + 0.06w_r^2/V_a > -1.2w_r - (0.56 - 0.72\delta_e)u_r w_r / V_a \quad (38)$$

Since δ_e and w_r are much smaller than u_r during a stable flight (37) and (38) holds during normal operation of the UAV. Throughout the simulations presented in Section 6, the values assumed by ζ_1 (with a $V_{a,\min} = 14$ [m/s]) fluctuates around 39.5 and never drops below 36.8. For ζ_3 , the fluctuation is around 183 with a minimum of 177. The requirement $\zeta_1 \zeta_3 - \zeta_2^2 > 0$ is difficult to analyze analytically but, the magnitude of ζ_2 never exceeds 20.2 and it is therefore evident that the requirement is fulfilled throughout the simulation. However, there exists combinations of u_r , w_r and δ_e , which can occur in other conditions that do not guarantee this condition to hold. Because of the constraint (37) and some approximations the stability results are local for the Aerosonde UAV. Consequently, it is recommended to use the nonlinear observer only for flight envelopes accurately described by the aircraft model and stable flights.

6. SIMULATION STUDY

To assess the effectiveness of the proposed nonlinear wind observer, two different simulations have been conducted using Matlab Simulink. The simulations have been based on the complete model of the small aircraft system for the Aerosonde UAV presented in Beard and McLain [2012] including the autopilot module. The wind is modeled as a constant wind field with added turbulence. The turbulence is generated as white noise filtered through a Dryden model, an approach presented by Langelaan et al. [2011] and also used by Beard and McLain [2012]. The Dryden transfer functions for the wind turbulence are given by

$$H_u(s) = \sigma_u \sqrt{\frac{2V_a}{L_u}} \frac{1}{s + V_a/L_u} \quad (39)$$

$$H_v(s) = \sigma_v \sqrt{\frac{3V_a}{L_v}} \frac{(s + V_a/(\sqrt{3}L_v))}{(s + V_a/L_u)^2} \quad (40)$$

$$H_w(s) = \sigma_w \sqrt{\frac{3V_a}{L_w}} \frac{(s + V_a/(\sqrt{3}L_w))}{(s + V_a/L_u)^2} \quad (41)$$

where σ_u , σ_v , σ_w and L_u , L_v , L_w are the turbulence intensities and spatial wavelengths along the vehicle frame axes. For the simulations the Dryden model has been implemented with a constant nominal airspeed $V_a = V_{a_0}$. The gust model used is for a low altitude, moderate turbulence gust with the parameters listed in Table 1. For

Table 1. Dryden gust model parameters used in simulation.

altitude	50	m
L_u, L_v	200	m
L_w	50	m
σ_u, σ_v	2.12	m/s
σ_w	1.4	m/s
V_{a_0}	14	m/s

assessing the simulation results, the focus will be on the estimates of the wind velocity and the AOA and SSA since these variables are of primary interest with respect to using the nonlinear wind observer in conjunction with a control system or fault detection module. During simulations the observer measurements have been used with the noise from Appendix H and Chapter 7 in Beard and McLain [2012] on IMU measurements, pitot static probe measurements and GNSS velocity measurements. For the GNSS velocity measurement noise a std. dev. of 0.05 m has been used. Since the noise on the estimate $\hat{\mathbf{v}}_w^b$ is proportional to the noise of the GNSS velocity measurement \mathbf{v}^n , the GNSS velocity measurement has been filtered through a simple observer. The observer gains are $K_\gamma = 4$ and $K_u = K_\gamma / u_r^m$.

6.1 Simulation study I

During the first simulation the aircraft autopilot control objectives are changed in steps. The aircraft control objectives start with an altitude of 50 m and an airspeed command of 26 m/s. After 30 seconds the course command control objective is increased by 10 degrees, where it stays for the next 30 seconds. At time 90 s, the altitude control objective is increased by 5 meters and once again decreased after 30 seconds. At time 150 s until time 180 s the speed control objective is increased from 26 m/s to 30 m/s. In the middle of the simulation after 100 seconds the airspeed measurement scaling factor γ steps from 1.0 to 1.1 to assess the scaling factor estimation capabilities of the observer. The wind velocity and wind velocity estimation is shown in Figure 2. The nonlinear wind observer displays excellent estimation capabilities for the wind velocity along the lateral axis of the aircraft. In the longitudinal and vertical directions the observer is still able to provide precise estimates of the wind velocity, but there appears to be a small delay. Figure 3 shows the real AOA and SSA variables along with the estimated ones, calculated directly from the estimated relative velocity, along with the

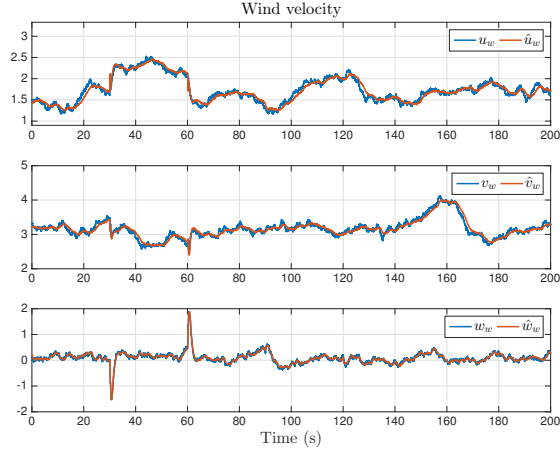


Fig. 2. Three plots showing the true values of the wind along with their respective estimates from a simulation with a maneuvering UAV.

airspeed measurement scaling factor. The wind observer displays great capability in estimating the AOA. With the SSA signal, which is noisy and centered around zero, it is harder to assess the quality of the estimate, but it appears to follow the tendencies of the real value during the moments of excitation. The airspeed measurement scaling factor estimation shows good estimation capabilities and converges quickly to the new value of the true variable.

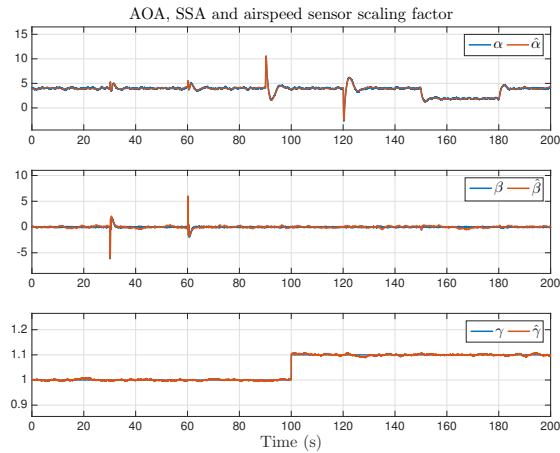


Fig. 3. Three plots showing the AOA, SSA and airspeed measurement scaling factor true variables and their respective estimates from a simulation with a maneuvering UAV.

6.2 Simulation study II

To assess the nonlinear wind observer under actuator uncertainties, the second simulation includes a 10% mismatch between values of the aircraft parameters in the wind observer for the thrust force created by the propeller actuator and the true model values. This is emulated as

$$\mathbf{f}_{p,model} = 1.1 \cdot \mathbf{f}_{p,true} \quad (42)$$

The simulation is conducted using the same autopilot control inputs as in Simulation I, but without the change

in scaling factor. The simulation results are shown in Figures 4 and 5. The nonlinear wind observer displays an offset in the longitudinal wind velocity estimation, while the estimates in the lateral and vertical directions have only degraded mildly. The AOA estimate also appears to be affected by a small offset, whereas the SSA estimates displays similar performance to the former simulation.

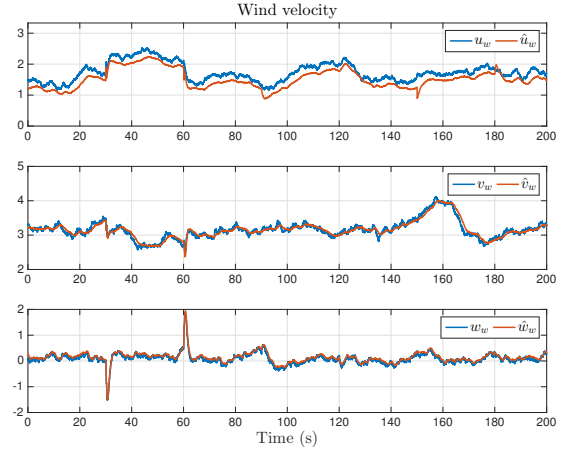


Fig. 4. Three plots showing the true values of the wind velocity along with their respective estimates from a simulation with an actuator uncertainty.

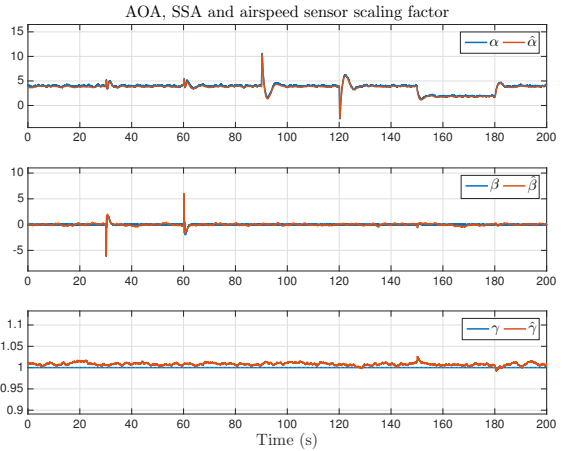


Fig. 5. Three plots showing the AOA, SSA and airspeed measurement scaling factor true variables and their respective estimates from a simulation with propulsion model uncertainty.

7. CONCLUSIONS

In this paper a nonlinear wind observer for a UAV was proposed. The wind observer combines a model of the aircraft with a GNSS-aided INS including an attitude observer and a pitot static probe. The nonlinear wind observer provides estimates of both the wind velocity and the relative velocity, from which the AOA and SSA are computable. The nonlinear wind observer developed does not have any requirements of PE of the aircraft. The nonlinear wind observer has been proven to be exponentially stable and is verified through simulation.

ACKNOWLEDGMENTS

This work was supported by the Norwegian Research Council (grant no. 221666 and 223254) through the Center of Autonomous Marine Operations and Systems (NTNU AMOS) at the Norwegian University of Science and Technology.

APPENDIX A

Lemma 1. (Aerodynamic forces). Under the assumptions stated in Section 4.2 the aerodynamic forces $\boldsymbol{\tau}_{\text{aero},1}(\mathbf{v}_r^b, t)$ in (20) can be expressed as the sum of a linear and nonlinear term according to:

$$\boldsymbol{\tau}_{\text{aero},1}(\mathbf{v}_r^b, t) = -\mathbf{D}(t)\mathbf{v}_r^b - \mathbf{d}(\mathbf{v}_r^b, t) \quad (43)$$

Proof: Defining the longitudinal wind speed

$$V_{\text{lon}} \triangleq \sqrt{u_r^2 + w_r^2} \quad (44)$$

By application of trigonometric relations

$$\sin(\alpha) = \sin\left(\tan^{-1}\left(\frac{w_r}{u_r}\right)\right) = \frac{w_r}{V_{\text{lon}}} \quad (45)$$

$$\cos(\alpha) = \cos\left(\tan^{-1}\left(\frac{w_r}{u_r}\right)\right) = \frac{u_r}{V_{\text{lon}}} \quad (46)$$

The following expressions for the aerodynamic forces are based on linear theory and the assumption that $V_a \approx V_{\text{lon}}$. Hence,

$$\beta = \sin^{-1}\left(\frac{v_r}{V_a}\right) \approx \frac{v_r}{V_a} \quad (47)$$

The linear sway force in (21) for an aircraft that is symmetrical about the xz -plane ($C_{Y_0} = 0$) then becomes:

$$C_{Y_0} + C_{Y_\beta}\beta = C_{Y_\beta}\frac{v_r}{V_a} \quad (48)$$

Furthermore

$$\alpha = \sin^{-1}\left(\frac{w_r}{V_{\text{lon}}}\right) \approx \frac{w_r}{V_a} \quad (49)$$

$$C_L(\alpha) \approx C_{L_0} + C_{L_\alpha}\alpha = C_{L_0} + C_{L_\alpha}\frac{w_r}{V_a} \quad (50)$$

$$C_D(\alpha) \approx C_{D_0} + C_{D_\alpha}\alpha = C_{D_0} + C_{D_\alpha}\frac{w_r}{V_a} \quad (51)$$

and

$$C_{X_{\delta_e}}(\alpha)\delta_e \triangleq (-C_{D_{\delta_e}}\cos(\alpha) + C_{L_{\delta_e}}\sin(\alpha))\delta_e \quad (52)$$

$$\approx (-C_{D_{\delta_e}}\frac{u_r}{V_a} + C_{L_{\delta_e}}\frac{w_r}{V_a})\delta_e \quad (53)$$

$$C_{Z_{\delta_e}}(\alpha)\delta_e \triangleq (-C_{D_{\delta_e}}\sin(\alpha) - C_{L_{\delta_e}}\cos(\alpha))\delta_e \quad (54)$$

$$\approx (-C_{D_{\delta_e}}\frac{w_r}{V_a} - C_{L_{\delta_e}}\frac{u_r}{V_a})\delta_e \quad (55)$$

Hence, with abuse of notation we define a function $\boldsymbol{\tau}_{\text{aero}}(\mathbf{v}_r^b, t)$, which depends on the state \mathbf{v}_r^b and several time-varying measurements all denoted by the single argument t as:

$$\begin{aligned} \boldsymbol{\tau}_{\text{aero},1}(\mathbf{v}_r^b, t) &:= \frac{1}{2}\rho S V_a^2 \begin{bmatrix} -C_D(\alpha)\cos(\alpha) + C_L(\alpha)\sin(\alpha) \\ C_{Y_0} + C_{Y_\beta}\beta \\ -C_D(\alpha)\sin(\alpha) - C_L(\alpha)\cos(\alpha) \end{bmatrix} \\ &+ \frac{1}{2}\rho V_a^2 \begin{bmatrix} C_{X_q}(\alpha)\frac{c}{2V_a}q + C_{X_{\delta_e}}(\alpha)\delta_e - \frac{1}{S}S_{\text{prop}}C_{\text{prop}} \\ 0 \\ C_{Z_q}(\alpha)\frac{c}{2V_a}q + C_{Z_{\delta_e}}(\alpha)\delta_e \end{bmatrix} \\ &= \frac{1}{2}\rho V_a^2 S \begin{bmatrix} -(C_{D_0} + C_{D_\alpha}\frac{w_r}{V_a})\frac{u_r}{V_a} + (C_{L_0} + C_{L_\alpha}\frac{w_r}{V_a})\frac{w_r}{V_a} \\ C_{Y_\beta}\beta \\ -(C_{D_0} + C_{D_\alpha}\frac{w_r}{V_a})\frac{w_r}{V_a} - (C_{L_0} + C_{L_\alpha}\frac{w_r}{V_a})\frac{u_r}{V_a} \end{bmatrix} \\ &+ \frac{1}{2}\rho V_a^2 S \begin{bmatrix} (-C_{D_q}\frac{u_r}{V_a} + C_{L_q}\frac{w_r}{V_a})\frac{c}{2V_a}q \\ 0 \\ (-C_{D_q}\frac{w_r}{V_a} - C_{L_q}\frac{u_r}{V_a})\frac{c}{2V_a}q \end{bmatrix} \\ &+ \frac{1}{2}\rho V_a^2 S \begin{bmatrix} (-C_{D_{\delta_e}}\frac{u_r}{V_a} + C_{L_{\delta_e}}\frac{w_r}{V_a})\delta_e - \frac{1}{S}S_{\text{prop}}C_{\text{prop}} \\ 0 \\ \frac{c}{2V_a}q + (-C_{D_{\delta_e}}\frac{w_r}{V_a} - C_{L_{\delta_e}}\frac{u_r}{V_a})\delta_e \end{bmatrix} \end{aligned} \quad (56)$$

Since the airspeed V_a will be positive for any values of \mathbf{v}_r^b we rewrite V_a as

$$V_a = V_{a,\text{min}} + \Delta V_a \quad (57)$$

Combining (56) and (57) we obtain

$$\begin{aligned} \boldsymbol{\tau}_{\text{aero},1}(\mathbf{v}_r^b, t) &= -\frac{1}{2}\rho S \underbrace{\begin{bmatrix} \sigma_1 & 0 & -\sigma_2 \\ 0 & -C_{Y_\beta} & 0 \\ \sigma_2 & 0 & \sigma_1 \end{bmatrix}}_{\mathbf{D}(t)} \begin{bmatrix} u_r \\ v_r \\ w_r \end{bmatrix} \\ &- \frac{1}{2}\rho S \underbrace{\begin{bmatrix} C_{D_\alpha}u_r w_r - C_{L_\alpha}w_r^2 + \frac{1}{S}S_{\text{prop}}C_{\text{prop}}V_a^2 + \eta_1\Delta V_a \\ 0 \\ C_{L_\alpha}u_r w_r + C_{D_\alpha}w_r^2 + \eta_2\Delta V_a \end{bmatrix}}_{\mathbf{d}(\mathbf{v}_r^b, t)} \end{aligned} \quad (58)$$

where

$$\sigma_1 \triangleq (C_{D_0} + C_{D_{\delta_e}}\delta_e)V_{a,\text{min}} + C_{D_q}cq(t)/2$$

$$\sigma_2 \triangleq (C_{L_0} + C_{L_{\delta_e}}\delta_e)V_{a,\text{min}} + C_{L_q}cq(t)/2$$

$$\eta_1 \triangleq (C_{D_0} + C_{D_{\delta_e}}\delta_e)u_r - (C_{L_0} + C_{L_{\delta_e}}\delta_e)w_r$$

$$\eta_2 \triangleq (C_{L_0} + C_{L_{\delta_e}}\delta_e)u_r + (C_{D_0} + C_{D_{\delta_e}}\delta_e)w_r$$

■

APPENDIX B

Proof: From theorem 4.14 in Khalil [2002] we know there exists a Lyapunov function $V_a(\tilde{\mathbf{R}}) : \mathbb{R}^{3 \times 3} \mapsto \mathbb{R}$ that satisfies:

$$\dot{V}_a \leq -c\|\tilde{\mathbf{R}}\|^2 \quad (59)$$

for some $c > 0$. With an attitude estimate, instead of a measurement, (26) should be replaced with:

$$\begin{aligned} m\dot{\hat{\mathbf{v}}}_r^b &= -\mathbf{S}(t)\hat{\mathbf{v}}_r^b + \boldsymbol{\tau}_{\text{aero},1}(\hat{\mathbf{v}}_r^b, t) + \boldsymbol{\tau}_{\text{aero},2}(t) \\ &- m\hat{\mathbf{R}}^\top(t)\mathbf{g}^n - K_u\mathbf{h}(\mathbf{h}^\top\hat{\mathbf{v}}_r^b - \hat{\gamma}u_r^m(t)) \end{aligned} \quad (60)$$

and the error dynamics instead becomes:

$$\begin{aligned} m\dot{\tilde{\mathbf{v}}}_r^b &= -\mathbf{D}(t)\tilde{\mathbf{v}}_r^b - (\mathbf{d}(\mathbf{v}_r^b, t) - \mathbf{d}(\hat{\mathbf{v}}_r^b, t)) \\ &+ K_u\mathbf{h}(u_r^m(t)\tilde{\gamma} - \mathbf{h}^\top\tilde{\mathbf{v}}_r^b) + m\tilde{\mathbf{v}}_r^{b\top}\hat{\mathbf{R}}^\top\mathbf{g}^n \end{aligned} \quad (61)$$

The time derivative of the Lyapunov function:

$$\begin{aligned} \dot{V} &\leq -[\tilde{\gamma} \ \tilde{\mathbf{v}}_r^{b\top}] \mathbf{Q} \begin{bmatrix} \tilde{\gamma} \\ \tilde{\mathbf{v}}_r^b \end{bmatrix} + m\tilde{\mathbf{v}}_r^{b\top} \tilde{\mathbf{R}}^\top \mathbf{g}^n \\ &\leq -\lambda_{\min}(\mathbf{Q})\|\tilde{\gamma}\|^2 - \lambda_{\min}(\mathbf{Q})\|\tilde{\mathbf{v}}_r^{b\top}\|^2 + mg\|\tilde{\mathbf{v}}_r^b\|\|\tilde{\mathbf{R}}\| \end{aligned} \quad (62)$$

where the time argument of \mathbf{Q} has been omitted for notational simplicity. Consider the augmented Lyapunov function

$$W(\tilde{\gamma}, \tilde{\mathbf{v}}_r^b, \tilde{\mathbf{R}}) = V(\tilde{\gamma}, \tilde{\mathbf{v}}_r^b) + \kappa V_a(\tilde{\mathbf{R}}) \quad (63)$$

where $\kappa > 0$. Hence,

$$\begin{aligned} \dot{W} &\leq -\lambda_{\min}(\mathbf{Q})\|\tilde{\gamma}\|^2 - \lambda_{\min}(\mathbf{Q})\|\tilde{\mathbf{v}}_r^{b\top}\|^2 \\ &\quad + mg\|\tilde{\mathbf{v}}_r^b\|\|\tilde{\mathbf{R}}\| - \kappa c\|\tilde{\mathbf{R}}\|^2 \\ &\leq -[\|\tilde{\mathbf{v}}_r^b\| \ \|\tilde{\mathbf{R}}\| \ \|\tilde{\gamma}\|] \mathbf{H} [\|\tilde{\mathbf{v}}_r^b\| \ \|\tilde{\mathbf{R}}\| \ \|\tilde{\gamma}\|]^\top \end{aligned} \quad (64)$$

where

$$\mathbf{H} = \begin{bmatrix} \lambda_{\min}(\mathbf{Q}) - \frac{1}{2}gm & 0 & 0 \\ -\frac{1}{2}gm & \kappa c & 0 \\ 0 & 0 & \lambda_{\min}(\mathbf{Q}) \end{bmatrix} \quad (65)$$

Hence, \mathbf{H} is positive definite since κ can always be chosen such that $\kappa > g^2m^2/(4\lambda_{\min}(\mathbf{Q})c)$. ■

REFERENCES

- Aamo, O.M., Arcak, M., Fossen, T.I., and Kokotovic, P.V. (2001). Global output tracking control of a class of Euler-Lagrange systems with monotonic non-linearities in the velocities. *International Journal of Control*, 74(7), 649–658.
- Beard, R.W. and McLain, T.W. (2012). *Small Unmanned Aircraft - Theory and Practice*. Princeton University Press.
- Brown, R.G. (1972). Integrated navigation systems and Kalman filtering: a perspective. *Journal of the Institute of Navigation*, 19, 355–362.
- Cho, A., Kang, Y., Park, B., and Yoo, C. (2013). Airflow angle and wind estimation using GPS/INS navigation data and airspeed. In *2013 13th International Conference on Control, Automation and Systems*, 1321–1324.
- Cho, A., Kim, J., Lee, S., and Kee, C. (2011). Wind estimation and airspeed calibration using a UAV with a single-antenna GPS receiver and pitot tube. *IEEE Transactions on Aerospace and Electronic Systems*, 47(1), 109–117.
- Farrell, J.A. (2008). *Aided Navigation: GPS with High Rate Sensors*. McGraw-Hill.
- Fossen, T.I. (2011). *Handbook of Marine Craft Hydrodynamics and Motion Control*. Wiley.
- Hansen, S. and Blanke, M. (2014). Diagnosis of airspeed measurement faults for unmanned aerial vehicles. *IEEE Transactions on Aerospace and Electronic Systems*, 50(1), 224–239.
- Johansen, T.A., Cristofaro, A., Sørensen, K.L., Hansen, J.M., and Fossen, T.I. (2015). On estimation of wind velocity, angle-of-attack and sideslip angle of small UAVs using standard sensors. In *2015 International Conference on Unmanned Aircraft Systems (ICUAS)*, 510–519. IEEE.
- Khalil, H.K. (2002). *Nonlinear Systems, Third Edition*. Prentice Hall.
- Kumon, M., Mizumoto, I., Iwai, Z., and Nagata, M. (2005). Wind Estimation by Unmanned Air Vehicle with Delta Wing. In *Proceedings of the 2005 IEEE International Conference on Robotics and Automation*, 1896–1901. IEEE.
- Langelaan, J.W., Alley, N., and Neidhoefer, J. (2011). Wind Field Estimation for Small Unmanned Aerial Vehicles. *Journal of Guidance, Control, and Dynamics*, 34(4), 1016–1030.
- Lie, F.A.P. and Gebre-Egziabher, D. (2013). Synthetic Air Data System. *Journal of Aircraft*, 50(4), 1234–1249.
- Long, H. and Song, S. (2009). Method of estimating angle-of-attack and sideslip angel based on data fusion. In *2009 2nd International Conference on Intelligent Computing Technology and Automation, ICICTA 2009*, volume 1, 641–644.
- Paces, P., Draxler, K., Hanzal, V., Censky, T., and Vasko, O. (2010). A combined angle of attack and angle of sideslip smart probe with twin differential sensor modules and doubled output signal. In *2010 IEEE Sensors*, 284–289. IEEE.
- Ramprasad, C. and Arya, H. (2012). Multistage-Fusion Algorithm for Estimation of Aerodynamic Angles in Mini Aerial Vehicle. *Journal of Aircraft*, 49(1), 93–100.
- Rhudy, M.B., Larrabee, T., Chao, H., Gu, Y., and Napolitano, M. (2013). UAV Attitude, Heading, and Wind Estimation Using GPS/INS and an Air Data System. In *AIAA Guidance, Navigation, and Control (GNC) Conference*. American Institute of Aeronautics and Astronautics, Reston, Virginia.
- Rodriguez, A., Andersen, E., Bradley, J., and Taylor, C. (2007). Wind Estimation Using an Optical Flow Sensor on a Miniature Air Vehicle. In *AIAA Guidance, Navigation and Control Conference and Exhibit*. American Institute of Aeronautics and Astronautics, Reston, Virginia.
- Wenz, A.W., Johansen, T.A., and Cristofaro, A. (2016). Combining model-free and model-based Angle of Attack estimation for small fixed-wing UAVs using a standard sensor suite. In *International Conference on Unmanned Aircraft Systems, submitted and accepted, Washington DC*.